

Highly efficient CD4+ T cell targeting and genetic recombination using engineered CD4+ cell-homing mRNA-LNPs

István Tombácz,¹ Dorottya Laczkó,¹ Hamna Shahnawaz,¹ Hiromi Muramatsu,¹ Ambika Natesan,¹ Amir Yadegari,¹ Tyler E. Papp,¹ Mohamad-Gabriel Alameh,¹ Vladimir Shuvaev,² Barbara L. Mui,³ Ying K. Tam,³ Vladimir Muzykantov,² Norbert Pardi,¹ Drew Weissman,¹ and Hamideh Parhiz¹

¹Division of Infectious Diseases, Perelman School of Medicine, University of Pennsylvania, Philadelphia, PA 19104, USA; ²Department of Pharmacology, Perelman School of Medicine, University of Pennsylvania, Philadelphia, PA 19104, USA; ³Acuitas Therapeutics, Vancouver, BC V6T 1Z3, Canada

Nucleoside-modified messenger RNA (mRNA)-lipid nanoparticles (LNPs) are the basis for the first two EUA (Emergency Use Authorization) COVID-19 vaccines. The use of nucleoside-modified mRNA as a pharmacological agent opens immense opportunities for therapeutic, prophylactic and diagnostic molecular interventions. In particular, mRNA-based drugs may specifically modulate immune cells, such as T lymphocytes, for immunotherapy of oncologic, infectious and other conditions. The key challenge, however, is that T cells are notoriously resistant to transfection by exogenous mRNA. Here, we report that conjugating CD4 antibody to LNPs enables specific targeting and mRNA interventions to CD4+ cells, including T cells. After systemic injection in mice, CD4-targeted radiolabeled mRNA-LNPs accumulated in spleen, providing ~30-fold higher signal of reporter mRNA in T cells isolated from spleen as compared with non-targeted mRNA-LNPs. Intravenous injection of CD4-targeted LNPs loaded with Cre recombinase-encoding mRNA provided specific dose-dependent loxP-mediated genetic recombination, resulting in reporter gene expression in about 60% and 40% of CD4+ T cells in spleen and lymph nodes, respectively. T cell phenotyping showed uniform transfection of T cell subpopulations, with no variability in uptake of CD4-targeted mRNA-LNPs in naive, central memory, and effector cells. The specific and efficient targeting and transfection of mRNA to T cells established in this study provides a platform technology for immunotherapy of devastating conditions and HIV cure.

INTRODUCTION

Modulation of immune cells through activation, inhibition or modification to alter their properties has become a popular and high-demand class of therapy, called immunotherapeutics. Today's immunotherapeutics largely rely on biological protein-based agents, which are expensive and challenging to manufacture,^{1,2} or require *ex vivo* modification of immune cells.^{3,4} Some examples include antibodies or cytokines for modulating immune cell function, monoclonal antibodies for redirecting immune function, genetic editing of T cells for

preventing viral infections, and chimeric antigen receptor (CAR) T cell therapy.⁵⁻⁷

One of the most relevant applications of cancer immunotherapeutics are CAR T cell therapies. Currently, CAR T cells are generated *ex vivo*, which is costly, as it requires extended cell culture in GMP cell processing facilities. Additionally, it is not a treatment option for patients with solid tumors, very low T cell counts, or settings requiring large-scale use.⁸⁻¹⁰ There is a vital need for development of *in vivo* T cell-targeted messenger RNA (mRNA) delivery systems for robust and rapid generation of CAR T cells. mRNA-based CAR T cell therapeutics could also provide a safer platform by reducing the risk of CAR T cell-induced toxicities, because of their transient nature, as well as avoiding the risk of genomic integration, when so desired.¹¹⁻¹⁴ Moreover, mRNA-based therapeutics could offer gene-editing tools for treating viral infections and cancer or correcting genetic defects, such as knocking out the C-C chemokine receptor 5 (CCR5) gene for preventing HIV infection of T cells^{15,16} or knocking out the programmed cell death-1 (PDCD-1) gene for engineering superior tumor-infiltrating lymphocytes (TILs).¹⁷

One of the key obstacles in development of mRNA-based immunotherapeutics is efficient *in vivo* delivery. Development of an efficient, safe and immune-cell-specific mRNA delivery system could lead to the introduction and widescale use of current and the generation of a new class of robust mRNA-based immunotherapeutics. We previously developed a PECAM-targeted mRNA-lipid nanoparticle (LNP) platform that effectively and specifically delivered mRNA to endothelial cells¹⁸, and a VCAM-targeted platform for delivery to

Received 27 November 2020; accepted 1 June 2021;
<https://doi.org/10.1016/j.ymthe.2021.06.004>.

Correspondence: Drew Weissman, Division of Infectious Diseases, Perelman School of Medicine, University of Pennsylvania, Philadelphia, PA 19104, USA.

E-mail: drewww@penncmedicine.upenn.edu

Correspondence: Hamideh Parhiz, Division of Infectious Diseases, Perelman School of Medicine, University of Pennsylvania, Philadelphia, PA 19104, USA.

E-mail: Hamideh.Parhiz@penncmedicine.upenn.edu



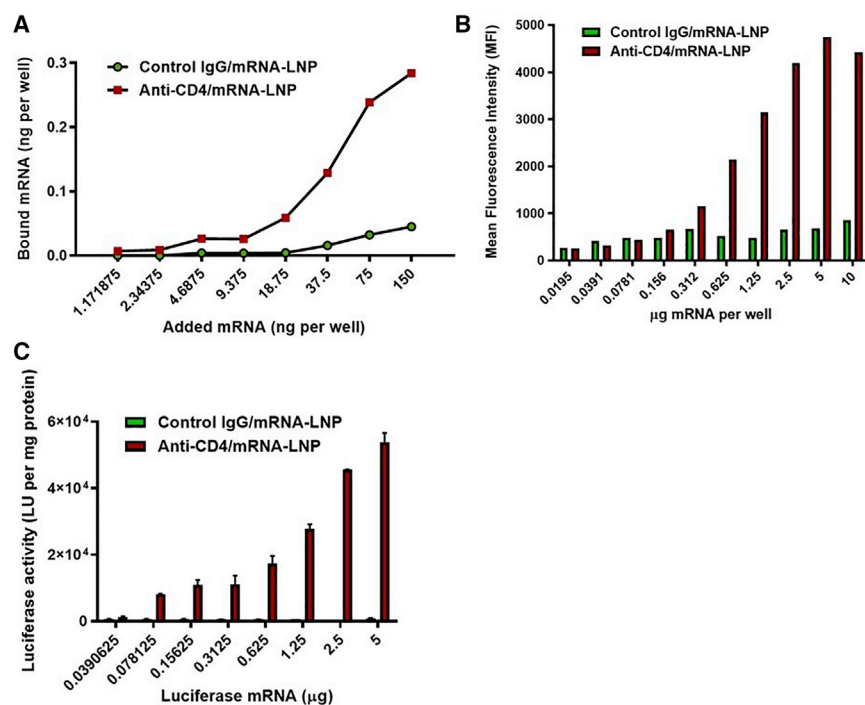


Figure 1. Binding and functional activity of CD4-targeted particles *in vitro*

(A) Specific *in vitro* binding of anti-human CD4⁺ T cells after 1 h incubation at room temperature (RT). (B) Binding of anti-CD4/mRNA-LNPs and control IgG/mRNA-LNPs to human CD4⁺ T cells, with increasing mRNA-LNP doses, and their corresponding mean fluorescence intensity (MFI). (C) Luc activity measured in human CD4⁺ T cells treated with anti-human CD4/mRNA-LNPs or control IgG/mRNA-LNPs.

LNPs or control IgG/Poly(C) RNA-LNPs, and fluorescein isothiocyanate (FITC)-tagged anti-rat IgG was used to monitor binding of antibody-conjugated LNPs to cells. Dose-responsive binding of anti-CD4/Poly(C) RNA-LNPs was observed.

In order to determine internalization and functional activity (mRNA translation) of the targeted mRNA-LNPs, anti-CD4 antibody- or control IgG-conjugated LNPs carrying firefly luciferase (Luc)-encoding mRNA were incubated with human CD4⁺ T cells. Efficient translation of the mRNA in cells targeted by anti-CD4/mRNA-LNPs was demonstrated compared to control IgG/mRNA-LNPs. Incubation of CD4⁺ T cells with higher doses of Luc mRNA-LNPd yielded higher Luc activity, demonstrating a dose-response correlation (Figure 1C).

In order to directly assess targeting efficiency on the single-cell level, and to test the targeting platform for gene-editing purposes, we next harvested splenocytes from mice harboring Ai6 (a Cre reporter allele with a loxP-flanked STOP cassette, which upon Cre-mediated recombination expresses robust ZsGreen1 fluorescence), and treated them with different amounts of targeted or non-targeted (unconjugated or control IgG-conjugated) Cre mRNA-LNPs. The cells were then collected and stained with antibodies against CD3 and CD8 (antibodies are listed in Table S1) and analyzed by flow cytometry. Gating strategy to identify ZsGreen1⁺ cells among the CD3⁺CD8⁻ population is presented in Figure 2B, with the corresponding ZsGreen1⁺ cells shown in Figure 2A. We used CD3⁺CD8⁻ staining instead of direct CD4 staining to identify CD4⁺ T cells because of the transient disappearance of CD4 upon administration of the anti-CD4 antibody-conjugated nanoparticles (Figure S1). A very low percentage of CD3⁺CD8⁻ cells exhibited positive ZsGreen1 signal when non-targeted LNPs were used, while approximately 80% of this cell population took up and translated Cre mRNA delivered in anti-CD4 antibody-conjugated LNPs, even at the lowest amount of mRNA-LNPs administered. We performed the same experiment on splenocytes harvested from Ai9 mice, which express robust tdTomato fluorescence following Cre-mediated recombination and

the inflamed brain.¹⁹ Here, we report on the development and evaluation of CD4-targeted LNPs containing nucleoside-modified mRNA for efficient and specific *in vitro* and *in vivo* delivery. The nucleoside-modified and purified (to remove double-stranded RNA [dsRNA]) mRNA used does not activate RNA sensors and does not induce type 1 IFNs and proinflammatory cytokines.^{20–22} Comprehensive radioactivity- or luminescence-based biodistribution analysis of CD4-targeted mRNA-LNPs demonstrates significant targeting of CD4⁺ T cells in lymphoid organs. The CD4-targeted mRNA-LNP platform induces potent and specific genetic editing using a Cre/loxP reporter system *in vivo*. The present nucleoside-modified mRNA-LNP platform offers a promising tool for *in vivo* T cell manipulation.

RESULTS

Anti-CD4/mRNA-LNPs target CD4⁺ T cells *in vitro*

Considering that T cells do not naturally endocytose nanoparticles, we initially examined surface antigens that endocytose after mAb or ligand binding, and selected CD4.²³ CD4 receptor targeting has also been shown to be capable of uptake and internalization upon nanoparticle binding.^{24,25} The binding capacity of the targeted mRNA-LNPs was first evaluated on human CD4⁺ T cells obtained from healthy donors. Anti-CD4 antibody (anti-CD4/mRNA-LNPs) or non-specific isotype control IgG (control IgG/mRNA-LNPs) was conjugated to LNPs. As shown in Figure 1A, radiolabeled anti-CD4/mRNA-LNPs selectively bound to human CD4⁺ T cells, while control IgG counterparts did not. Selective targeting to CD4⁺ T cells was also confirmed using flow cytometry (Figures 1B). Human CD4⁺ T cells were incubated with either anti-CD4/Poly(C) RNA-

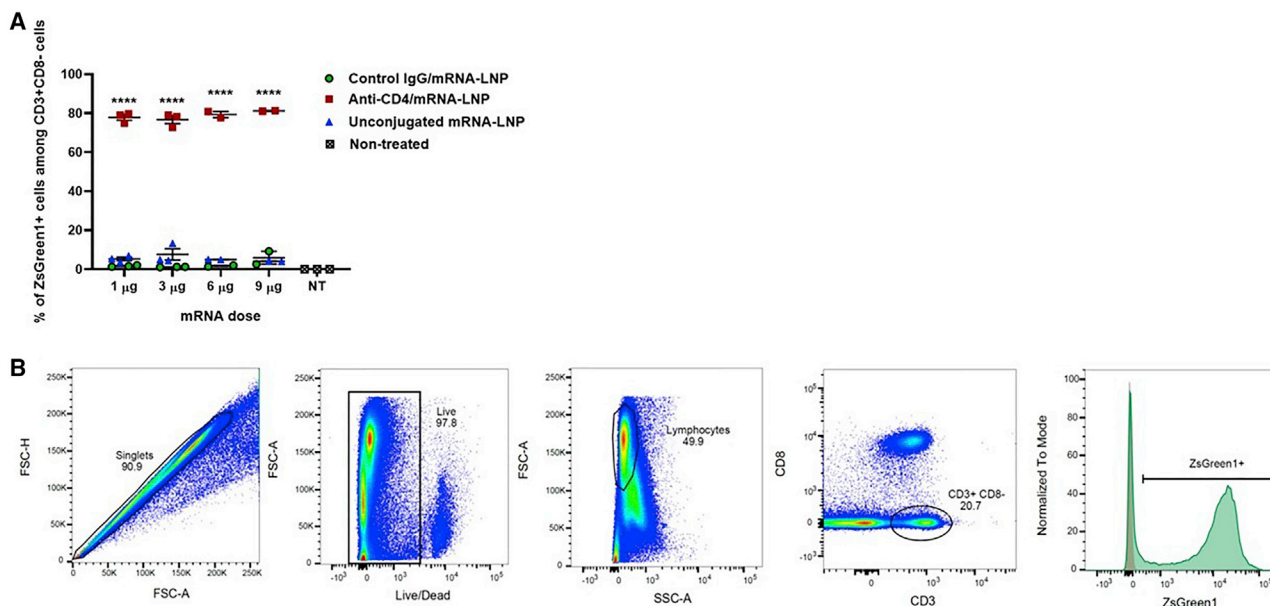


Figure 2. Cre mRNA-mediated genetic recombination *in vitro*

(A) Cre mRNA-induced genetic recombination and consequent reporter gene expression presented as % of ZsGreen1⁺ cells among CD3⁺CD8⁻ cells. Splenocytes were harvested from Ai6 mice and incubated with Cre mRNA-LNPs at doses of 1, 3, 6, or 9 µg per 2 million cells. %ZsGreen1⁺ cells upon anti-CD4/mRNA-LNP administration was compared to control IgG/mRNA-LNP and unconjugated mRNA-LNP administration (mean with SEM is shown; ****p < 0.0001, two-way ANOVA with Bonferroni correction). (B) Gating strategy to identify ZsGreen1⁺ cells among CD3⁺CD8⁻ cells.

obtained similar results (data not shown). This shows the potential of the targeted anti-CD4/mRNA-LNPs to efficiently transfect CD4⁺ T cells *in vitro*.

Anti-CD4/mRNA-LNPs target CD4⁺ T cells *in vivo*

We next analyzed the biodistribution of anti-CD4/mRNA-LNPs in mice after retro-orbital intravenous (i.v.) administration. LNPs were directly labeled with ¹²⁵I prior to conjugation with anti-mouse CD4 or control IgG; therefore, measured radioactivity only showed distribution of particles without any detached targeting antibodies affecting the outcome. To measure tissue uptake, the amount of radioactivity in various tissues (percent of injected dose per gram of tissue: %ID/g) was calculated.

As expected, a substantial number of control IgG/mRNA-LNPs were still circulating in the blood (19.35%ID/g ± 2.2%ID/g) 0.5 h post injection, representing a significant change in the biodistribution with a reduction in liver targeting of control IgG/LNPs (Figure 3A). For anti-CD4/mRNA-LNPs, lower numbers of particles were circulating (10.84%ID/g ± 0.42%ID/g). The majority of the anti-CD4/mRNA-LNP uptake occurred in the spleen (131.59%ID/g ± 9.71%ID/g), representing a 3.5-fold increase in splenic uptake compared to the control IgG/mRNA-LNPs (37.6%ID/g ± 8.67%ID/g). The localization ratio (LR), defined as the ratio of %ID/g of a given organ to that in the blood, was also calculated for both CD4-targeted and control IgG/mRNA-LNPs. The spleen being part of the reticuloendothelial system contributes to non-spe-

cific splenic uptake that is observed with the untargeted mRNA-LNPs. Anti-CD4/mRNA-LNPs were localized in spleen at a 6-fold higher level than their control IgG counterparts (Figure 3B; Figure S2A).

To further explore and quantitate the kinetics of *in vivo* tissue uptake of anti-CD4/mRNA-LNPs, targeted and non-targeted ¹²⁵I-labeled poly(C) RNA-LNPs were injected i.v. into mice. Groups of animals were sacrificed at 0.5, 1, and 24 h after injection, and selected tissues (blood, spleen, liver, lung, and kidneys) were harvested. The highest circulating amount of targeted mRNA-LNPs was 10.84%ID/g ± 0.42%ID/g in blood at the earliest time point tested (Figure 3C). At later time points, the concentration of targeted particles in blood quickly dropped to a %ID/g of 6.86 ± 1.34 and 0.51 ± 0.07 at 1 and 24 h, respectively. Specific splenic uptake of targeted particles peaked at 0.5 h post injection (131.59%ID/g ± 9.71%ID/g) (Figure 3C), and the localization ratio increased over time, reaching to 61.15 at the last time point tested, 24 h (Figure 3D).

mRNA in targeted LNPs is efficiently delivered to CD4⁺ T cells *in vivo*

mRNA translation after i.v. administration of Luc mRNA-LNPs was then analyzed in mice. Control IgG/Luc mRNA-LNPs and anti-CD4/Luc mRNA-LNPs were first administered at a dose of 8 µg (0.32 mg/kg) mRNA. Five hours after injection, various organs were harvested, and luciferase activity was either measured from tissue lysates or was detected by direct luminescent imaging of whole

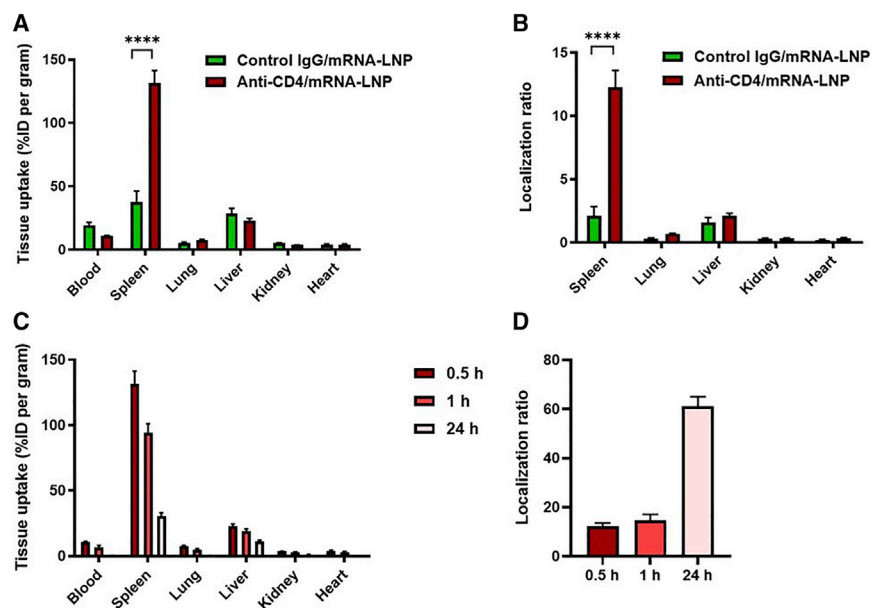


Figure 3. Targeting of mRNA-LNP to CD4⁺ cells *in vivo*

(A) Biodistribution of ¹²⁵I-labeled anti-CD4/ and control IgG/poly(C) RNA-LNPs in mice at 0.5 h. Tissue uptake is indicated as mean ± SEM (****p < 0.0001). (B) Localization ratio, calculated as the ratio of %ID/g of a given organ to that in the blood of mice treated with either ¹²⁵I-labeled anti CD4/ or control IgG/mRNA-LNP at 30 min post-injection. Mean ± SEM is shown. *In vivo* mRNA-LNP binding as quantitative measurement of the percentage of radiolabeled anti-CD4/mRNA-LNPs in selected organs (C) and localization ratios in spleens (D), after intravenous injection of mRNA-LNPs. Group size is 3 animals. Statistical analysis was performed by two-way ANOVA with Bonferroni correction (****p < 0.0001).

organs (Figures 4A–4C). The Luc expression pattern showed a marked difference between anti-CD4 and control IgG/Luc mRNA-LNP-treated mice, as the luminescence signal decreased significantly in liver with CD4 targeting. Most importantly, Luc activity for anti-CD4/Luc-mRNA-LNPs was ~7-fold higher compared to the control IgG-modified mRNA-LNPs in the spleen (Figures 4A and 4B). After removal of the spleen, kidneys, lungs, heart, and liver—which exhibits high uptake of both unconjugated and antibody-conjugated LNPs—we were able to observe lymph node luciferase expression in the anti-CD4/Luc mRNA-LNP-treated mice (Figure 4C). This shows the capacity of targeted LNPs to traverse endothelial membranes and functionally access cells in tissues, such as lymph nodes.

To demonstrate that we delivered mRNA specifically to the T cell population, we isolated CD3⁺ T cells (as CD4 selection could not be performed) from the spleen of mice treated as above. Luc activity of the CD3⁺ population after anti-CD4/Luc mRNA-LNP administration was 33-fold higher than in control IgG/Luc mRNA-LNP-treated samples. We concluded that with Luc activity concentrated in T cells (Figure 4D), CD4⁺ T cells are being specifically and efficiently targeted after i.v. delivery of targeted nanoparticles.

To confirm the targeting efficiency of the CD4-targeted mRNA-LNP platform with LNP formulations other than ALC-0307 LNPs, we applied the same antibody conjugation strategy on the Acuitas LNP formulation containing the ionizable lipid 0315 (ALC-0315 LNP), which is the LNP formulation in the recently US Food and Drug Administration (FDA)-approved Pfizer/BioNTech COVID vaccine.^{26,27} The list of ingredients in this LNP formulation is provided in Table S2. Five hours after injection of anti-CD4-targeted Luc mRNA-ALC-0315 LNPs, we

observed a very similar Luc expression pattern to CD4-targeted ALC-0307 LNPs (i.e., a higher luminescence signal in the spleen and a lower signal in liver) (Figure S3) when compared to control IgG counterparts. These data prove that we can achieve similar targeting efficiency with CD4 targeting of other LNP formulations, such as ALC-0315 LNP.

CD4-targeted Cre-mRNA-LNPs mediate genetic recombination in CD4⁺ T cells *in vivo*

A principal use for targeted mRNA therapy would be gene editing and insertion to express therapeutic proteins or correct genetic deficiencies. To evaluate the efficiency of delivery of mRNA using CD4-targeted LNPs at the cellular level for *in vivo* genetic modification, we administered Cre mRNA-LNPs to Ai6 mice (Figure 5A). In these mice, the Cre/loxP-mediated expression of a reporter gene encoding the fluorescent protein ZsGreen1 allows for easy readout of successfully transfected and LoxP-recombined target cells using flow cytometry (Figures 5B and 5C). A wide range of doses (3, 10, 30, and 90 μg) were tested. Mice were injected i.v., then spleens and lymph nodes were harvested the next day, and single-cell suspensions were prepared from each tissue. Cells were stained for flow cytometry using antibodies against CD3 and CD8 to identify CD4⁺ T cells (Table S1). No signal was observed in non-treated animals, indicating no leakage of the reporter construct. Administration of control IgG/Cre mRNA-LNPs led to low efficiency of transfection, similar in level over the range of mRNA doses we used, in both tissues tested (i.e., spleens [Figure 5B] and lymph nodes [Figure 5C]). A significant increase in the number of ZsGreen1-expressing cells was observed with anti-CD4/Cre mRNA-LNP treatment at all tested mRNA doses when compared to control IgG- and unconjugated mRNA-LNP counterparts (Figures 5B and 5C). In mice treated with unconjugated mRNA-LNPs, we observed a substantial increase in mRNA delivery and subsequent Cre/loxP recombination (up to approximately 20% of ZsGreen1⁺ cells in the CD3⁺CD8⁻ cell population) when we increased the dose to 30 μg. This is still well below the strong response we observed with targeted mRNA-LNPs at all tested doses and is

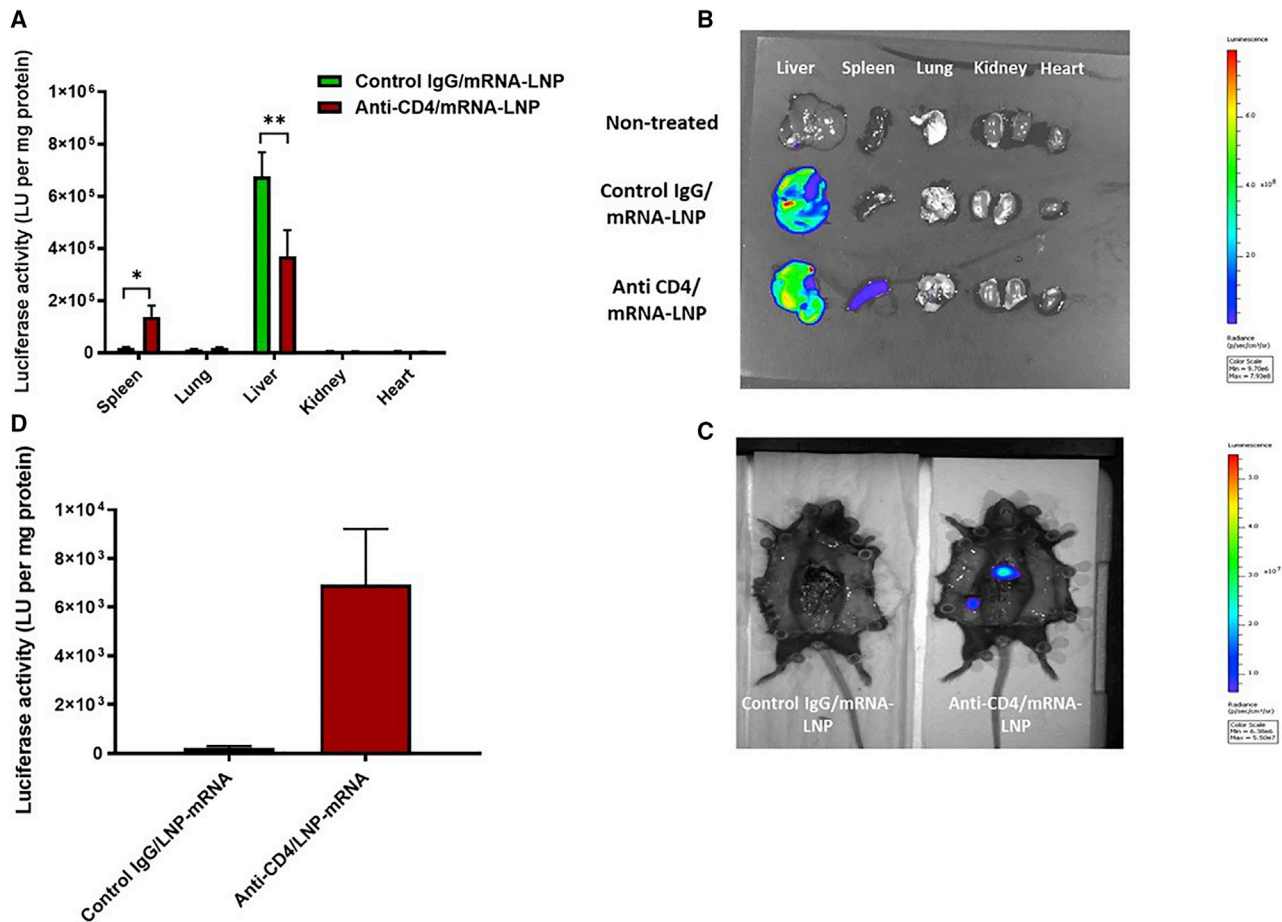


Figure 4. Biodistribution of targeted mRNA-LNP expression *in vivo*

Mice were *i.v.* injected with 8 μ g of mRNA-LNPs. Organ distribution of Luc mRNA expression 5 h after administration of anti-CD4/ and control IgG/Luc mRNA-LNP was evaluated by (A) measuring Luc activity in lysed tissues and by (B and C) luminescence imaging. (A) Quantitative expression of Luc as light unit (LU)/mg protein. A representative sample set of dissected mouse organs (B) and whole carcasses after organ removal (showing luminescing lymph nodes) (C) were analyzed 5 min after the administration of D-luciferin. (D) Quantitative expression of Luc as LU/mg protein values in CD3⁺ cell preparation obtained from the spleens of mice injected with the mRNA-LNPs. (A and D) Error bars indicate SEM. Group size is 3 animals. Statistical analysis was performed by two-way ANOVA with Bonferroni correction, (* $p < 0.05$, ** $p < 0.01$, and *** $p < 0.001$).

likely due to expression of an ApoE receptor by some T cells.^{28,29} While administration of 90 μ g of anti-CD4/Cre mRNA-LNPs resulted in an even higher percentage of ZsGreen1⁺ CD4⁺ T cells (not shown), this amount of LNPs proved to be toxic in all groups (both unconjugated and control IgG-conjugated, and CD4-targeted LNP treatments); thus, we eliminated that dose from further experiments. This was not a surprise, since cationic lipids are well known to cause toxicity at high doses.³⁰ Selective CD4 targeting versus control of untargeted LNPs did not increase the uptake of nanoparticles in macrophages and dendritic cells (Figure S4), likely due to their extensive natural phagocytic uptake of nanoparticles, whereas with CD4⁺ T cells, there is significant increase in targeted mRNA-LNP uptake compared to untargeted control mRNA-LNPs. The number of ZsGreen1-expressing cells in non-T cell splenocytes, such as dendritic cells and macrophages, did not differ among the range of doses in this study (Figure S4).

A similar experiment was performed using CD4-targeted ALC-0315 LNPs. When we *i.v.* injected Ai6 mice with these targeted LNPs carrying Cre mRNA, targeting efficiency comparable to CD4-targeted ALC-0307 LNP-Cre mRNA was observed (increase in the number of ZsGreen1-expressing cells in mice treated with anti-CD4/ALC-0315 LNP-Cre mRNA treatment compared to control IgG counterparts) (Figure S5).

CD4⁺ T cell targeting with anti-CD4/mRNA-LNPs is not T cell-subtype specific

We investigated whether the uptake of the targeted LNPs was favored by certain T cell subtypes. One day after the administration of a 10 μ g dose of Cre mRNA-LNPs, spleens were harvested, and single-cell suspensions were stained with antibodies against CD3, CD8, CD44, and CD62L to identify naive, memory, and effector memory T cell subpopulations. We found no significant preference for the CD4-targeted

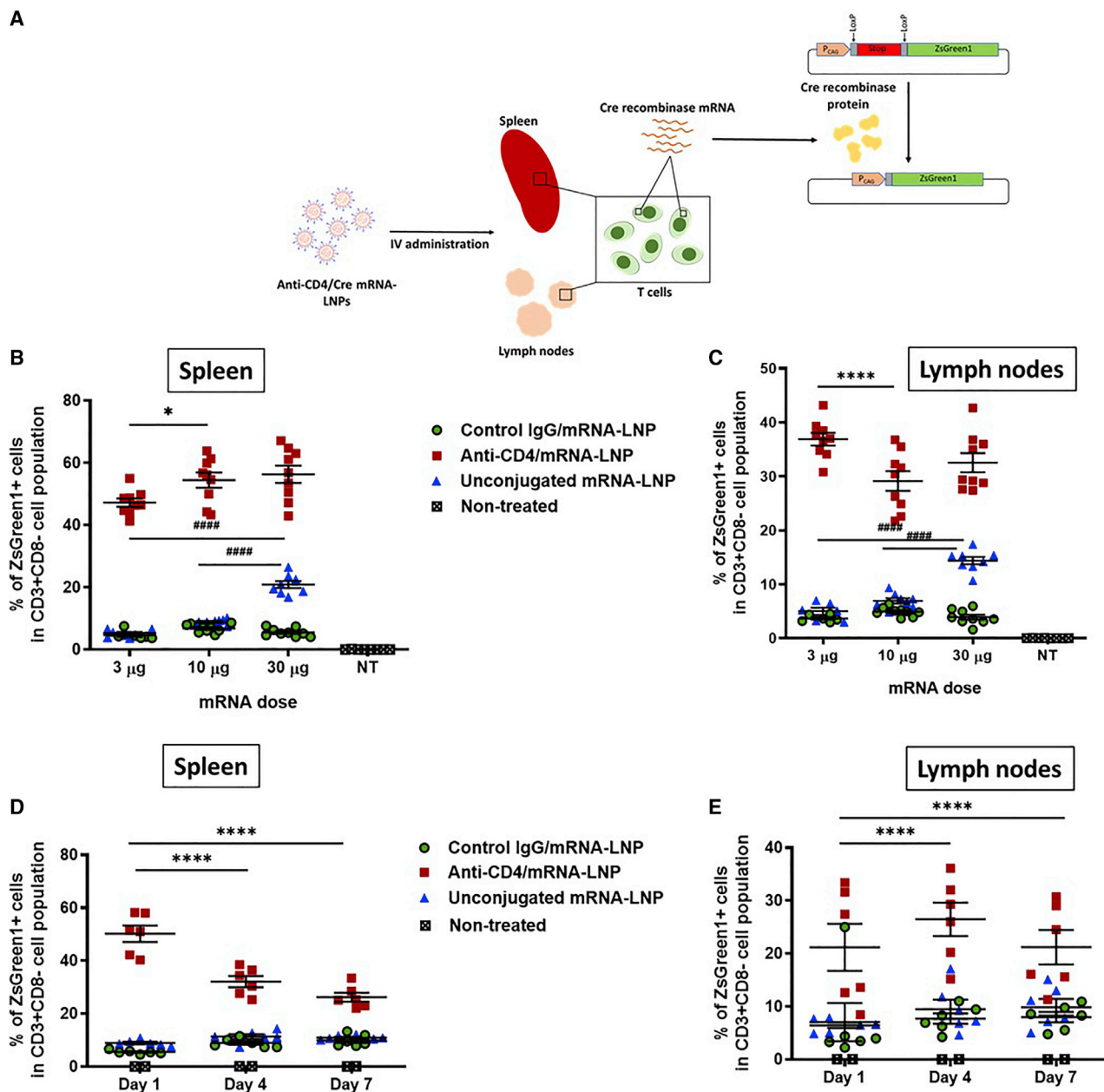


Figure 5. Cre-mediated genetic recombination upon *in vivo* administration of CD4-targeted Cre mRNA-LNPs

(A) Schematic diagram depicting targeted delivery of anti-CD4/mRNA-LNPs for selective genetic recombination in CD4⁺ T cells, and the principle of the Ai6 reporter allele: Cre-mediated excision of a loxP-flanked STOP cassette allows robust expression of ZsGreen1, a fluorescent protein. Ai6 mice received Cre mRNA-LNPs at doses of 3, 10, and 30 µg via i.v. administration. Spleens and lymph nodes were harvested at 24 h post treatment and % of ZsGreen1⁺ cells in the CD3⁺CD8⁻ cell population were determined in splenic (B) and lymph node (C) single-cell suspensions using flow cytometry. Changes in the number of ZsGreen1-expressing CD4⁺ T cells in spleens (D) and lymph nodes (E) over time were monitored after i.v. injection of 10 µg of mRNA-LNPs. Group size is 8 or 9 (B and C) or 6 (D and E) animals in a total of three independent experiments. Each symbol represents one animal, and horizontal lines show the mean with SEM. Statistical analysis was performed by two-way ANOVA with Bonferroni correction. %ZsGreen1⁺ cells after injection of different doses of anti-CD4/mRNA-LNPs (* $p < 0.05$, **** $p < 0.0001$) and unconjugated mRNA-LNP (#### $p < 0.0001$) were compared.

mRNA-LNPs to be taken up and expressed by any specific CD4⁺ T cell subpopulation examined: CD4⁺ naive T cells (CD44⁻CD62L⁻), central memory T cells (CD44⁺CD62L⁺), and effector memory T cells (CD44⁺

CD62L⁻) (Figure 6A). The majority of T cells *in vivo* are not activated. We analyzed the expression of the T cell activation marker (CD25) on the CD4⁺ T cells receiving Cre mRNA-LNPs. Notably, CD4-targeted

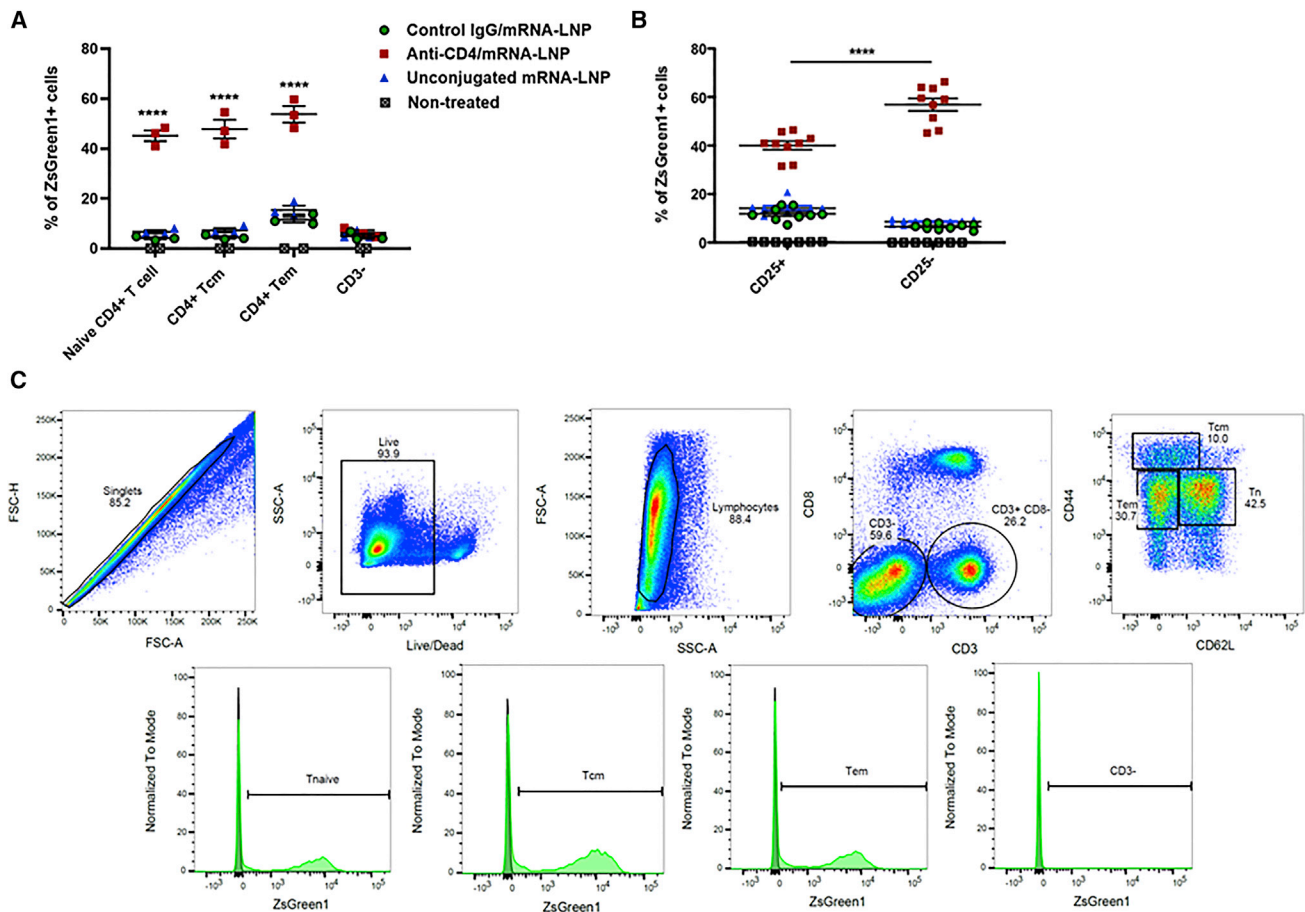


Figure 6. *In vivo* uptake of Cre mRNA-LNP by different T cell subtypes

Spleens were harvested at 24 h post-treatment with 10 μg of Cre mRNA-LNPs, and % of ZsGreen1⁺ cells in CD4⁺ T cell subpopulations (A) and versus CD25 marker (B) were determined using flow cytometry. Naive CD4⁺ T cells are considered as CD44⁺CD62L⁻, central memory T cells as CD44⁺CD62L⁺, and effector memory T cells as CD44⁺CD62L⁻. Group size is 3–11 animals. Each symbol represents one animal, and horizontal lines show the mean with SEM. Statistical analysis was performed by two-way ANOVA with Bonferroni correction comparing T cell subtypes (**p < 0.01, ****p < 0.0001). (C) Gating strategy to identify ZsGreen1⁺ cells among different CD4⁺ T cell subtypes.

mRNA-LNPs induced Cre recombination in ~57% of resting (CD25⁻), compared to ~40% of activated (CD25⁺) CD4⁺ T cells (Figure 6B), thus demonstrating efficient targeting, transfection, and gene recombination in resting CD4⁺ T cells.

Number of recombined cells decreases over time after CD4-targeted delivery in the spleen

ZsGreen1 expression was tracked for 7 days after a single i.v. administration of 10 μg of Cre mRNA-LNPs. Spleens and lymph nodes were harvested 1, 4, or 7 days post-injection, and single-cell preparations were stained for flow cytometric analysis as above. Four days after administration of 10 μg of anti-CD4/Cre mRNA-LNPs, the number of ZsGreen1-expressing splenic CD4⁺ T cells dropped significantly (from ~50% at day 1 to ~32% at day 4). However, it held at a similar level of around 26% at the last time point tested (day 7), still significantly above the values observed with IgG and unconjugated counterparts (Figure 5D). Blood and spleen are sites of transient-recirculating

T cells, which these data reflect.^{31,32} The ZsGreen1 expression for all treatments did not significantly change over 7 days in T cells extracted from lymph nodes (Figure 5E). This reflects the longer residence time of T cells in lymph nodes.^{31,32}

***In vivo* targeted mRNA-LNP-induced specific genetic recombination shows an additive effect**

We also tested the potential additive effect of targeted mRNA delivery by serial administrations of mRNA-LNPs (Figures 7A and 7B). Mice received three or five i.v. injections of 10 μg doses of Cre mRNA-LNPs, one injection every 24 h. Spleens and lymph nodes were harvested the day after the last injection. Five injections resulted in a significantly higher number of ZsGreen1⁺ cells when compared to three injections. Interestingly, a steady increase in ZsGreen1-expressing CD4⁺ T cell numbers was observed for both control IgG/ and unconjugated mRNA-LNPs. However, the expression increased to 28% in the unconjugated group, still relatively lower than the anti-CD4/

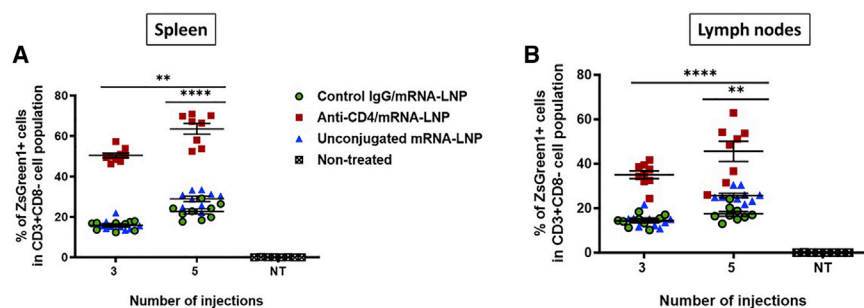


Figure 7. mRNA-LNP targeting efficiency using multiple administrations

Ai6 mice received 10 μ g (0.4 mg/kg) of anti-CD4/, control IgG/, or unconjugated Cre mRNA-LNPs via i.v. administration as daily injections for 3 or 5 days. Spleens and lymph nodes were harvested after three or five sequential injections, and the % of ZsGreen1⁺ cells in the CD3⁺CD8⁻ cell population was determined in splenic (A) and lymph node (B) single-cell suspensions using flow cytometry. Group size is 9 animals. Each symbol represents one animal, and horizontal lines show the mean. Error bars indicate SEM. Statistical analysis was performed by two-way ANOVA with Bonferroni correction. % ZsGreen1⁺ cells after different number of injections of anti-CD4/mRNA-LNP (** $p < 0.01$, **** $p < 0.0001$) were compared with unconjugated mRNA-LNP.

mRNA-LNPs at any number of injections tested. Overall, the sequential administrations of the targeted mRNA-LNPs resulted in increasing Cre-induced genetic recombination with increased number of injections in both the spleen and lymph nodes.

DISCUSSION

mRNA-based therapeutics offer numerous advantages that address challenges with the current protein- or viral-based immunotherapy approaches, such as difficult manufacturing, instability, lack of control over amount and duration of expression, high toxicity, and, in some cases, genomic integration or off-site effects.^{33–35} Efficient *in vivo* delivery has been the key obstacle in development of mRNA-based immunotherapeutics. To date, T cell modification for clinical application has required extraction of autologous T cells, expansion, and genomic editing *ex vivo*, which is expensive and time-consuming and precludes widespread use for more common diseases, such as HIV.

T cells are known as hard-to-transfect cells.^{25,36,37} Here, we demonstrated that targeting human T cells with anti-CD4 antibody-conjugated Luc mRNA-LNPs, but not with control IgG-conjugated LNPs, resulted in strong binding and luciferase expression in human CD4⁺ T cells in a dose-dependent manner (Figures 1A–1C). Similarly, when injected systemically into C57BL/6 mice, anti-mouse CD4/mRNA-LNPs specifically accumulated, and the mRNA was translated in T cell-enriched tissues, such as spleen and lymph nodes (Figures 3 and 4A–4C). Furthermore, we functionally evaluated the potential of our T cell-targeted mRNA-LNP system to mediate genome editing using a Cre/loxP reporter system. We were able to successfully induce Cre-mediated genetic recombination in CD4⁺ T cells *in vivo*. Interestingly, the signal from non-targeted mRNA-LNPs in both splenic and lymphatic tissues at high dose (30 μ g per mouse) was not zero, as observed in untreated mice. This observation is likely due to expression of an ApoE receptor by certain T cells,^{28,29} as LNPs bind ApoE and typically target the liver.³⁸ We could further increase the percentage of gene-edited cells by multiple injections of anti-CD4/mRNA-LNPs. This high level of *in vivo* T cell-targeted genetic recombination has not been reported elsewhere. An important finding for potential gene-editing therapies was that similar levels of gene recombination

were observed in resting and activated CD4⁺ T cells. Evaluation of the presence of successfully targeted T cells over time showed a gradual decrease of ZsGreen1 signal in spleen during 1 week post-treatment with anti-CD4/mRNA-LNPs. This trend was expected, considering the lifespan of circulatory T cells, which are a predominant population of T cells in spleen.^{39,40} However, ZsGreen1 expression in lymph nodes remained minimally changed over the 7-day experiment time after treatment with anti-CD4/mRNA-LNPs. A report analyzing the migration of ⁵¹Cr-labeled thoracic duct lymphocytes (TDLs) in major lymphoid and non-lymphoid tissues of rats revealed that lymphocytes have longer residence time in the lymph nodes than the spleen.³¹ Comparable residence times were reported for mice as well.³² Finally, we evaluated if various T cell subtypes differed in being targeted. There was no significant difference in uptake and recombination among naive, memory, and effector memory subtypes when treated with anti-CD4/Cre mRNA-LNPs.

Our anti-CD4/LNP-mRNA system allows for CD4⁺ T cell targeting in the tissues, such as spleen and lymph nodes, which is critical for T cell therapies. Our current T cell-targeting platform has great potential for many *in vivo* T cell manipulation-based applications by making T cell-targeted therapeutic mRNA delivery possible. *In vivo* delivery to specific cell types (e.g., T lymphocytes, among others) is an intensely developing field, evidenced by many recent studies.^{41–45} LNPs modified with antibodies have been used for delivery of small interfering RNA (siRNA) to lymphocytes for gene silencing purposes. Ramishetti et al.⁴⁶ surface modified siRNA-loaded LNPs with anti-CD4 monoclonal antibodies for targeting CD4⁺ T lymphocytes. They observed gene silencing in approximately 30% of CD4⁺ T cells isolated from spleen, which is only half of the targeted functional activity we observed with our CD4-targeted Cre mRNA-LNPs (~60% of CD4⁺ T cells in spleen). It is of note that because of their use of siRNA-LNPs and the non-binary readout of their experiments, direct comparison of targeting efficiencies of the two platforms is not straightforward. Other attempts have been made for lymphocyte targeting with other lipid- and polymer-based carriers. McKinlay et al.⁴⁷ reported on a combinatorial chemical approach of mRNA delivery using hybrid lipid-based amphiphilic charge-altering releasable transporters (CARTs), achieving approximately 1.5% T

lymphocyte transfection efficiency in mice. Similarly, Fenton et al.⁴³ described specific LNP design for delivering mRNA to B lymphocytes without using active targeting ligand. They showed an enhanced luminescence signal from the B cell targeted-Luc mRNA-LNP formulation in spleen compared to other non-selective formulations of their LNP formulation library. Veiga et al.⁴⁵ delivered mRNA in surface-modified LNPs to inflammatory Ly6C⁺ leukocytes using their ASSET platform, which also employs monoclonal antibody targeting. Delivery and expression of mRNA encoding IL-10 showed significant therapeutic effect in a colitis model. While some T cells also express Ly6c, as do monocytes, macrophages, and neutrophils, it was not determined which populations of leukocytes take up and express Ly6c-targeted LNPs and to what extent. To our knowledge, our targeted mRNA-LNP platform is the first report of an LNP-based mRNA delivery system for selective and functional CD4⁺ targeting.

Overall, the CD4-targeted mRNA-LNP platform presented here offers tremendous opportunity for a wide range of *in vivo* T cell manipulations. The great potential of this system to reach all T cell subtypes in difficult-to-access tissues, such as lymph nodes, will make the targeting platform available for many types of T cell manipulation *in vivo*. The application potentials include delivering mRNA therapeutics to T cells for potential HIV cure. In particular, targeted delivery of engineered genomic editing enzymes have the potential to cure HIV, by excising the HIV integrated provirus from the genome of latently infected cells.⁴⁸ Additionally, targeted modification of lymphocytes has numerous applications for development of fast-acting and cost-effective immunotherapeutics for a range of cancers, infectious diseases, and immunological disorders.

MATERIALS AND METHODS

Ethics statement

The investigators faithfully adhered to the Guide for the Care and Use of Laboratory Animals by the Committee on Care of Laboratory Animal Resources Commission on Life Sciences, National Research Council.

Mice

Mouse studies were conducted under protocols approved by the University of Pennsylvania (UPenn) Institutional Animal Care and Use Committee. The animal facilities at the University of Pennsylvania are fully accredited by the American Association for Assessment and Accreditation of Laboratory Animal Care.

C57BL/6J mice

Equal numbers of male and female C57BL/6J mice were purchased from Jackson Laboratory.

Ai6 (RCL-ZsGreen) mice

Ai6 (RCL-ZsGreen) mice on C57BL/6J background were purchased from Jackson Laboratory (stock no: 007906) and bred homozygous in-house. Ai6 is a Cre reporter allele with a loxP-flanked STOP cassette preventing transcription of a CAG promoter-driven enhanced green fluorescent protein variant (ZsGreen1), all inserted

into the Gt(ROSA)26Sor locus. Upon Cre-mediated recombination, Ai6 mice express robust ZsGreen1 fluorescence.

mRNA production and LNP preparation

Coding sequences of Cre recombinase or firefly luciferase were codon-optimized, synthesized, and cloned into the mRNA production plasmid (pUC-ccTEV-Cre-A101 and pUC-ccTEV-Luc2-A101, respectively). mRNAs were produced using T7 RNA polymerase (Megascript, Ambion) on linearized plasmids. mRNAs were transcribed to contain 101-nucleotide-long poly(A) tails. m1 Ψ -5'-triphosphate (TriLink) instead of UTP was used to generate modified nucleoside-containing mRNA. Capping of the *in vitro* transcribed mRNA was performed co-transcriptionally using the trinucleotide cap1 analog, CleanCap (TriLink). mRNA was purified by cellulose purification, as described.⁴⁹ All mRNAs were analyzed by native agarose gel electrophoresis and were stored frozen at -20°C .

m1 Ψ -containing mRNAs were encapsulated in LNPs using a self-assembly process in which an aqueous solution of mRNA at pH 4.0 is rapidly mixed with a solution of lipids dissolved in ethanol.⁵⁰ LNPs used in this study were similar in composition to those described previously,^{50,51} which contain an ionizable cationic lipid (proprietary to Acuitas)/phosphatidylcholine/cholesterol/PEG-lipid (50:10:38.5:1.5 mol/mol) and were encapsulated at an RNA to total lipid ratio of ~ 0.04 (wt/wt).

Unless otherwise mentioned, Acuitas LNPs containing the ionizable lipid ALC-0307 (ALC-0307 LNP) were used for the experiments. Poly(C) RNA (Sigma-Aldrich, cat. no. P4903) was used as mRNA replacement in experiments when we traced carrier behavior, and we did not aim to measure mRNA activity.

Monoclonal antibody-conjugated LNPs

LNPs were conjugated with monoclonal antibodies (mAbs) specific for CD4. Purified NA/LE Rat anti-mouse CD4 (BD PharMingen), purified rat anti-human CD4 antibody, clone A161A1 (BioLegend), and control isotype-matched IgG were coupled to LNPs via SATA (N-succinimidyl S-acetylthioacetate)-maleimide conjugation chemistry, as described earlier.¹⁸ Briefly, LNPs were modified with DSPE-PEG-maleimide micelle by a modified post-insertion technique. The antibody was modified with SATA (Sigma-Aldrich) to introduce sulfhydryl groups allowing conjugation to maleimide. SATA was deprotected using 0.5 M hydroxylamine followed by removal of the unreacted components by G-25 Sephadex Quick Spin Protein columns (Roche Applied Science, Indianapolis, IN, USA). The reactive sulfhydryl group on the antibody was then conjugated to maleimide moieties using thioether conjugation chemistry. Purification was performed using Sepharose CL-4B gel filtration columns (Sigma-Aldrich). mRNA content was calculated by performing a modified Quant-iT RiboGreen RNA assay (Invitrogen). LNPs were frozen at -80°C prior to addition of targeting ligands. After addition of the targeting ligand, all the targeted and non-targeted LNP preparations were kept at 4°C and were used within 3 days after preparation.

Particle size measurements were carried out in PBS (pH 7.4) at 25°C using dynamic light scattering (DLS) on a Malvern Zetasizer Nano ZS (Malvern Instruments, Worcestershire, UK). Diameters of unconjugated and antibody-conjugated mRNA-LNPs were interpreted as normalized intensity size distribution for particle preparations. The diameter of the unconjugated nanoparticles was ~80 nm. To evaluate antibody conjugation efficiency to LNPs, fluorescently labeled LNPs and antibodies were monitored throughout conjugation steps. Antibody-conjugated particles had a hydrodynamic diameter of 88.37 ± 4.2 with narrow size distribution (PDI = 0.1) and contained ~3.5 antibodies per LNP.

***In vitro* cell-binding studies**

For cell binding studies using radioactivity measurements, LNPs were first radiolabeled with Na¹²⁵I using Iodination Beads (Pierce) as described earlier.⁵² Human CD4⁺ T cells (obtained from the Human Immunology Core at University of Pennsylvania) were then incubated with increasing quantities of either anti-CD4/ or control IgG/RNA-LNPs for 1 h at room temperature. Incubation medium was then removed, and cells were washed with PBS buffer three times to remove the unbound nanoparticles from the cell surface. The cells were lysed with 1% Triton X-100 in 1 N NaOH, and the cell-associated radioactivity was measured by a Wallac 1470 Wizard gamma counter (Gaithersburg, MD, USA) and compared to total added activity.

For cell-binding studies using flow cytometry, human CD4⁺ T cells were seeded at 150,000 cells per well in 24-well plates. LNPs carrying Poly(C) RNA were added to the media at increasing quantities of RNA per well, and cells were incubated for 1 h at room temperature. Incubation medium was then removed, and cells were washed with PBS buffer three times to remove the unbound nanoparticles from the cell surface. FITC-tagged anti-rat IgG (Abcam, Cambridge, UK) was used to monitor binding of antibody-conjugated LNPs on a BD LSR II flow cytometer.

***In vitro* cell transfection studies**

For cell transfection studies using firefly luciferase mRNA, human CD4⁺ T cells were plated in 48-well plates. After 18 h, LNPs carrying reporter luciferase mRNA were added at increasing concentrations to the cells and incubated for 1.5 h. Plates were then washed three times with PBS, and complete medium was added to the cells. After culturing for 24 h in complete media, cells were washed with PBS, lysed in luciferase cell culture lysis reagent (Promega, Madison, WI, USA), and the luciferase enzymatic activity as luminescence (Luciferase assay system, Promega) was measured.¹⁸ Transfections were performed in triplicate.

For cell transfection studies using Cre recombinase mRNA, spleens from two Ai6 mice were harvested, and a pooled single-cell suspension was produced. 2 million splenocytes were then plated in each well of 6-well plates. Cells were incubated with 1, 3, 6, or 9 μg of CD4-targeted or non-targeted (unconjugated or control IgG-conjugated) Cre mRNA-LNPs overnight. Cells were then collected and

stained with Live/Dead Aqua (Thermo Fisher Scientific, L34966) and antibodies against CD3 and CD8 (and CD4, which was omitted from later experiments; see Figure S1), and the percentage of ZsGreen1-expressing CD3⁺CD8⁻ cells was determined using flow cytometry.

Biodistribution of anti-CD4/mRNA-LNPs in C57BL/6J mice: tissue uptake

¹²⁵I-radiolabeled mRNA-LNPs were administered by i.v. (retro-orbital) injection into C57BL/6 mice (Jackson Laboratory, Bar Harbor, ME, USA). Blood was collected at 0.5, 1, and 24 h post-injection from the inferior vena cava. Specific organs (liver, spleen, lung, kidney, and heart) were also harvested at the same time points, rinsed with saline, blotted dry, and weighed. The amount of radioactivity in each organ as well as in 100 μL samples of blood was measured in a gamma counter (Wallac 1470 Wizard gamma counter, Gaithersburg, MD, USA). Tissue uptake as %ID/g and localization ratio as organ-to-blood ratio were calculated using radioactivity values and weight of the samples. Immunospecificity index (ISI) was also calculated as the ratio of the LR of CD4-targeted mRNA-LNPs to that of control IgG-modified ones.

Biodistribution of anti-CD4/mRNA-LNPs in C57BL/6J mice: luciferase mRNA translation at tissue and cellular level

C57BL/6J mice were i.v. (retro-orbital) injected with anti-CD4/mRNA-LNP or control IgG/mRNA-LNP formulations. At 5 h after injection, animals were euthanized, and selected organs (liver, spleen, lung, kidney and heart) were harvested, rinsed with PBS, and stored at -80°C until analysis. When thawed, tissue samples were homogenized in appropriate volumes of cell lysis buffer (1×) (Promega Corp, Madison, WI, USA) containing protease inhibitor cocktail (1×) and mixed gently at 4°C for 1 h. The homogenates were then subjected to cycles of freeze/thaw in dry ice/37°C and centrifuged for 10 min at 16,000 g at 4°C. Luciferase activity was then measured in the supernatant using a Victor 3 1420 Multilabel Plate Counter (Perkin Elmer, Wellesley, MA, USA). We further analyzed the mRNA expression in the CD3⁺ cell population. CD3⁺ cells were isolated from the spleens or lymph nodes of injected mice using the MagniSort Mouse CD3⁺ Selection Kit (Thermo Fisher Scientific, Waltham, MA, USA) based on manufacturer's instructions. Briefly, a biotinylated anti-mouse CD3 antibody and streptavidin-coated magnetic beads were utilized for CD3⁺ cell isolation. CD3⁺ cells were bound to the antibody and then to magnetic beads. When placed in a magnetic field, the undesired cells were separated from CD3⁺ cells by decanting. Luciferase activity measurements were performed on the cell lysate of the CD3⁺-enriched cell population.

Bioluminescence imaging

C57BL/6J mice were i.v. (retro-orbital) injected with anti-CD4/mRNA-LNP or control IgG/mRNA-LNP formulations. At 5 h after injection, bioluminescence imaging was carried out as described previously¹⁸ using an IVIS Spectrum imaging system (Caliper Life Sciences, Waltham, MA, USA). D-luciferin was administered to mice

intraperitoneally at a dose of 150 mg/kg. After 5 min, the mice were euthanized; desired tissues were harvested and immediately placed on the imaging platform. Tissue luminescence was measured on the IVIS imaging system using an exposure time of 5 s or longer to ensure that the signal obtained was within operative detection range. Bioluminescence values were also quantified by measuring photon flux (photons/s) in the region of interest using LivingImage software provided by Caliper.

Determination of targeting efficiency of anti-CD4/mRNA-LNP using a Cre/loxP reporter system

To analyze delivery efficiency to targeted cell populations within the spleen and lymph nodes, mRNA translation was tracked with single-cell resolution. The targeted and non-targeted LNPs containing Cre recombinase mRNA were i.v. (retro-orbital) injected into Ai6 mice carrying a Cre reporter allele with a loxP-flanked STOP cassette preventing transcription of a green fluorescent protein variant (ZsGreen1). Cre recombinase excises the loxP-flanked STOP cassette, therefore allowing the transcription of ZsGreen1. At desired time points after injection, animals were euthanized, and spleens and lymph nodes were harvested. The number of CD3⁺CD8⁻ cells emitting green fluorescent signal in organ single-cell suspensions was evaluated using flow cytometry.

Single-cell suspension preparation and flow cytometry

Single-cell suspensions were prepared from spleens and lymph nodes. Briefly, the tissues were crushed using the frosted end of glass microscope slides and then passed through a 70- μ m filter. Following centrifugation and removal of supernatant, cells were resuspended in RPMI + 10% FBS medium and were first stained with Live/Dead Aqua cell stain (Thermo Fisher Scientific, cat. no. L34957), then a mixture of anti-mouse antibodies (Table S1). The stained single-cell populations were characterized on a BD LSR II flow cytometer (BD Biosciences). 500,000 events were collected per sample. Compensation of multicolor flow was carried out using ArC Amine Reactive beads (Thermo Fisher Scientific) for Live/Dead Aqua, Compbead anti-Rat, and anti-Hamster Ig κ /Negative Control Compensation Particles set (BD Biosciences) for all antibodies, and GFP BrightComp eBeads (Thermo Fisher Scientific, cat. no. A10514) for ZsGreen1. Data were analyzed with FlowJo software (Ashland, OR, USA).

Data availability

The authors declare that all data supporting the results of this study are available within the paper and its supplemental information files. Source data collected in this study are available from the corresponding author upon request.

SUPPLEMENTAL INFORMATION

Supplemental information can be found online at <https://doi.org/10.1016/j.ymthe.2021.06.004>.

ACKNOWLEDGMENTS

We thank the Human Immunology Core at University of Pennsylvania for providing human T cells for the experiments. H.P. was sup-

ported by a grant from the Penn Center for AIDS Research (CFAR), an NIH-funded program (P30 AI 045008). D.W. received funding from the NIH (HL134839 and AI124429).

AUTHOR CONTRIBUTIONS

H.P. and D.W. conceived and directed the project. H.P., I.T., and N.P. designed the experiments. I.T., D.L., H.S., H.M., A.N., A.Y., and T.E.P. performed most of experiments. M.G.A. and V.S. helped with some experiments. B.L.M. and Y.K.T. designed and formulated the unmodified mRNA-LNPs. H.P. and I.T. conducted the data analysis and interpreted the results. H.P. wrote the paper. D.W. and V.M. helped with the review and editing process. All authors read and approved the final manuscript.

DECLARATION OF INTERESTS

H.P., I.T., N.P., V.R.M., and D.W. are inventors on a patent filed on some aspects of this work. Those interests have been fully disclosed to the University of Pennsylvania. All other authors declare no competing interests.

REFERENCES

- Pranchevicius, M.C., and Vieira, T.R. (2013). Production of recombinant immunotherapeutics for anticancer treatment: the role of bioengineering. *Bioengineered* 4, 305–312.
- Liu, M., and Guo, F. (2018). Recent updates on cancer immunotherapy. *Precis. Clin. Med.* 1, 65–74.
- Schultz, L., and Mackall, C. (2018). Immunotherapy with Genetically Modified T Cells. In *Immunotherapy in Translational Cancer Research*, L.J.N. Cooper, E.A. Mittendorf, and J. Moyes, eds. (John Wiley & Sons), pp. 101–114.
- Maugeri, M., Nawaz, M., Papadimitriou, A., Angerfors, A., Camponeschi, A., Na, M., Hölttä, M., Skantze, P., Johansson, S., Sundqvist, M., et al. (2019). Linkage between endosomal escape of LNP-mRNA and loading into EVs for transport to other cells. *Nat. Commun.* 10, 4333.
- Schlake, T., Thess, A., Thran, M., and Jordan, I. (2019). mRNA as novel technology for passive immunotherapy. *Cell. Mol. Life Sci.* 76, 301–328.
- Wraith, D.C. (2017). The Future of Immunotherapy: A 20-Year Perspective. *Front. Immunol.* 8, 1668.
- Whilding, L.M., and Maher, J. (2015). CAR T-cell immunotherapy: The path from the by-road to the freeway? *Mol. Oncol.* 9, 1994–2018.
- Schmidts, A., and Maus, M.V. (2018). Making CAR T Cells a Solid Option for Solid Tumors. *Front. Immunol.* 9, 2593.
- Zhao, L., and Cao, Y.J. (2019). Engineered T Cell Therapy for Cancer in the Clinic. *Front. Immunol.* 10, 2250.
- Junghans, R.P. (2017). The challenges of solid tumor for designer CAR-T therapies: a 25-year perspective. *Cancer Gene Ther.* 24, 89–99.
- Foster, J.B., Barrett, D.M., and Karikó, K. (2019). The Emerging Role of In Vitro-Transcribed mRNA in Adoptive T Cell Immunotherapy. *Mol. Ther.* 27, 747–756.
- Foster, J.B., Choudhari, N., Perazzelli, J., Storm, J., Hofmann, T.J., Jain, P., Storm, P.B., Pardi, N., Weissman, D., Waanders, A.J., et al. (2019). Purification of mRNA Encoding Chimeric Antigen Receptor Is Critical for Generation of a Robust T-Cell Response. *Hum. Gene Ther.* 30, 168–178.
- Kowalski, P.S., Rudra, A., Miao, L., and Anderson, D.G. (2019). Delivering the Messenger: Advances in Technologies for Therapeutic mRNA Delivery. *Mol. Ther.* 27, 710–728.
- Pardi, N., Hogan, M.J., Porter, F.W., and Weissman, D. (2018). mRNA vaccines - a new era in vaccinology. *Nat. Rev. Drug Discov.* 17, 261–279.
- Didigu, C.A., Wilen, C.B., Wang, J., Duong, J., Secreto, A.J., Danet-Desnoyers, G.A., Riley, J.L., Gregory, P.D., June, C.H., Holmes, M.C., and Doms, R.W. (2014).

- Simultaneous zinc-finger nuclease editing of the HIV coreceptors *ccr5* and *cxcr4* protects CD4⁺ T cells from HIV-1 infection. *Blood* 123, 61–69.
16. Liu, Z., Chen, S., Jin, X., Wang, Q., Yang, K., Li, C., Xiao, Q., Hou, P., Liu, S., Wu, S., et al. (2017). Genome editing of the HIV co-receptors CCR5 and CXCR4 by CRISPR-Cas9 protects CD4⁺ T cells from HIV-1 infection. *Cell Biosci.* 7, 47.
 17. Bailey, S.R., and Maus, M.V. (2019). Gene editing for immune cell therapies. *Nat. Biotechnol.* 37, 1425–1434.
 18. Parhiz, H., Shuvaev, V.V., Pardi, N., Khoshnejad, M., Kiseleva, R.Y., Brenner, J.S., Uhler, T., Tuyishime, S., Mui, B.L., Tam, Y.K., et al. (2018). PECAM-1 directed re-targeting of exogenous mRNA providing two orders of magnitude enhancement of vascular delivery and expression in lungs independent of apolipoprotein E-mediated uptake. *J. Control. Release* 291, 106–115.
 19. Marcos-Contreras, O.A., Greineder, C.F., Kiseleva, R.Y., Parhiz, H., Walsh, L.R., Zuluaga-Ramirez, V., Myerson, J.W., Hood, E.D., Villa, C.H., Tombacz, I., et al. (2020). Selective targeting of nanomedicine to inflamed cerebral vasculature to enhance the blood-brain barrier. *Proc. Natl. Acad. Sci. USA* 117, 3405–3414.
 20. Karikó, K., Buckstein, M., Ni, H., and Weissman, D. (2005). Suppression of RNA recognition by Toll-like receptors: the impact of nucleoside modification and the evolutionary origin of RNA. *Immunity* 23, 165–175.
 21. Karikó, K., and Weissman, D. (2007). Naturally occurring nucleoside modifications suppress the immunostimulatory activity of RNA: implication for therapeutic RNA development. *Curr. Opin. Drug Discov. Devel.* 10, 523–532.
 22. Karikó, K., Muramatsu, H., Welsh, F.A., Ludwig, J., Kato, H., Akira, S., and Weissman, D. (2008). Incorporation of pseudouridine into mRNA yields superior nonimmunogenic vector with increased translational capacity and biological stability. *Mol. Ther.* 16, 1833–1840.
 23. Pitcher, C., Höning, S., Fingerhut, A., Bowers, K., and Marsh, M. (1999). Cluster of differentiation antigen 4 (CD4) endocytosis and adaptor complex binding require activation of the CD4 endocytosis signal by serine phosphorylation. *Mol. Biol. Cell* 10, 677–691.
 24. Cao, S., Jiang, Y., Levy, C.N., Hughes, S.M., Zhang, H., Hladik, F., and Woodrow, K.A. (2018). Optimization and comparison of CD4-targeting lipid-polymer hybrid nanoparticles using different binding ligands. *J. Biomed. Mater. Res. A* 106, 1177–1188.
 25. Peer, D. (2010). Induction of therapeutic gene silencing in leukocyte-implicated diseases by targeted and stabilized nanoparticles: a mini-review. *J. Control. Release* 148, 63–68.
 26. Thran, M., Mukherjee, J., Pönisch, M., Fiedler, K., Thess, A., Mui, B.L., Hope, M.J., Tam, Y.K., Horscroft, N., Heidenreich, R., et al. (2017). mRNA mediates passive vaccination against infectious agents, toxins, and tumors. *EMBO Mol. Med.* 9, 1434–1447.
 27. Ansell, S.M., and Du, X. (2017). Novel Lipids and Lipid Nanoparticle Formulations for Delivery of Nucleic Acids. Patent WO2017075531A1, filed October 28, 2016, and published May 4, 2017, <https://patents.google.com/patent/WO2017075531A1/en>.
 28. Sundqvist, K.G. (2018). T Cell Co-Stimulation: Inhibition of Immunosuppression? *Front. Immunol.* 9, 974.
 29. Panezai, J., Bergdahl, E., and Sundqvist, K.G. (2017). T-cell regulation through a basic suppressive mechanism targeting low-density lipoprotein receptor-related protein 1. *Immunology* 152, 308–327.
 30. Inglt, C.T., Sorri, A.J., Kuruppu, T., Vig, S., Cicalo, J., Ahmad, H., and Huang, H.C. (2020). Immunological and Toxicological Considerations for the Design of Liposomes. *Nanomaterials (Basel)* 10, 190.
 31. Ganusov, V.V., and Auerbach, J. (2014). Mathematical modeling reveals kinetics of lymphocyte recirculation in the whole organism. *PLoS Comput. Biol.* 10, e1003586.
 32. Mandl, J.N., Liou, R., Klauschen, F., Vrisekoop, N., Monteiro, J.P., Yates, A.J., Huang, A.Y., and Germain, R.N. (2012). Quantification of lymph node transit times reveals differences in antigen surveillance strategies of naive CD4⁺ and CD8⁺ T cells. *Proc. Natl. Acad. Sci. USA* 109, 18036–18041.
 33. Goswami, R., Subramanian, G., Silayeva, L., Newkirk, I., Doctor, D., Chawla, K., Chattopadhyay, S., Chandra, D., Chilukuri, N., and Betapudi, V. (2019). Gene Therapy Leaves a Vicious Cycle. *Front. Oncol.* 9, 297.
 34. Das, S.K., Menezes, M.E., Bhatia, S., Wang, X.-Y., Emdad, L., Sarkar, D., and Fisher, P.B. (2015). Gene Therapies for Cancer: Strategies, Challenges and Successes. *J. Cell. Physiol.* 230, 259–271.
 35. Chames, P., Van Regenmortel, M., Weiss, E., and Baty, D. (2009). Therapeutic antibodies: successes, limitations and hopes for the future. *Br. J. Pharmacol.* 157, 220–233.
 36. Gust, T.C., Neubrandt, L., Merz, C., Asadullah, K., Zügel, U., and von Bonin, A. (2008). RNA interference-mediated gene silencing in murine T cells: in vitro and in vivo validation of proinflammatory target genes. *Cell Commun. Signal.* 6, 3.
 37. Goffinet, C., and Keppler, O.T. (2006). Efficient nonviral gene delivery into primary lymphocytes from rats and mice. *FASEB J.* 20, 500–502.
 38. Akinc, A., Querbes, W., De, S., Qin, J., Frank-Kamenetsky, M., Jayaprakash, K.N., Jayaraman, M., Rajeev, K.G., Cantley, W.L., Dorkin, J.R., et al. (2010). Targeted delivery of RNAi therapeutics with endogenous and exogenous ligand-based mechanisms. *Mol. Ther.* 18, 1357–1364.
 39. Langeveld, M., Gamadia, L.E., and ten Berge, I.J.M. (2006). T-lymphocyte subset distribution in human spleen. *Eur. J. Clin. Invest.* 36, 250–256.
 40. Bronte, V., and Pittet, M.J. (2013). The spleen in local and systemic regulation of immunity. *Immunity* 39, 806–818.
 41. Veiga, N., Diesendruck, Y., and Peer, D. (2020). Targeted lipid nanoparticles for RNA therapeutics and immunomodulation in leukocytes. *Adv. Drug Deliv. Rev.* 159, 364–376.
 42. Mizrahy, S., Hazan-Halevy, I., Dammes, N., Landesman-Milo, D., and Peer, D. (2017). Current Progress in Non-viral RNAi-Based Delivery Strategies to Lymphocytes. *Mol. Ther.* 25, 1491–1500.
 43. Fenton, O.S., Kauffman, K.J., Kaczmarek, J.C., McClellan, R.L., Jhunjhunwala, S., Tibbitt, M.W., Zeng, M.D., Appel, E.A., Dorkin, J.R., Mir, F.F., et al. (2017). Synthesis and Biological Evaluation of Ionizable Lipid Materials for the In Vivo Delivery of Messenger RNA to B Lymphocytes. *Adv. Mater.* 29, 1606944.
 44. Ramishetti, S., Landesman-Milo, D., and Peer, D. (2016). Advances in RNAi therapeutic delivery to leukocytes using lipid nanoparticles. *J. Drug Target.* 24, 780–786.
 45. Veiga, N., Goldsmith, M., Granot, Y., Rosenblum, D., Dammes, N., Kedmi, R., Ramishetti, S., and Peer, D. (2018). Cell specific delivery of modified mRNA expressing therapeutic proteins to leukocytes. *Nat. Commun.* 9, 4493.
 46. Ramishetti, S., Kedmi, R., Goldsmith, M., Leonard, F., Sprague, A.G., Godin, B., Gozin, M., Cullis, P.R., Dykxhoorn, D.M., and Peer, D. (2015). Systemic Gene Silencing in Primary T Lymphocytes Using Targeted Lipid Nanoparticles. *ACS Nano* 9, 6706–6716.
 47. McKinlay, C.J., Benner, N.L., Haabeth, O.A., Waymouth, R.M., and Wender, P.A. (2018). Enhanced mRNA delivery into lymphocytes enabled by lipid-varied libraries of charge-altering releasable transporters. *Proc. Natl. Acad. Sci. USA* 115, E5859–E5866.
 48. Karpinski, J., Hauber, I., Chemnitz, J., Schäfer, C., Paszkowski-Rogacz, M., Chakraborty, D., Beschoner, N., Hofmann-Sieber, H., Lange, U.C., Grundhoff, A., et al. (2016). Directed evolution of a recombinase that excises the provirus of most HIV-1 primary isolates with high specificity. *Nat. Biotechnol.* 34, 401–409.
 49. Baiersdörfer, M., Boros, G., Muramatsu, H., Mahiny, A., Vlatkovic, I., Sahin, U., and Karikó, K. (2019). A Facile Method for the Removal of dsRNA Contaminant from In Vitro-Transcribed mRNA. *Mol. Ther. Nucleic Acids* 15, 26–35.
 50. Maier, M.A., Jayaraman, M., Matsuda, S., Liu, J., Barros, S., Querbes, W., Tam, Y.K., Ansell, S.M., Kumar, V., Qin, J., et al. (2013). Biodegradable lipids enabling rapidly eliminated lipid nanoparticles for systemic delivery of RNAi therapeutics. *Mol. Ther.* 21, 1570–1578.
 51. Jayaraman, M., Ansell, S.M., Mui, B.L., Tam, Y.K., Chen, J., Du, X., Butler, D., Eltepu, L., Matsuda, S., Narayanannair, J.K., et al. (2012). Maximizing the potency of siRNA lipid nanoparticles for hepatic gene silencing in vivo. *Angew. Chem. Int. Ed. Engl.* 51, 8529–8533.
 52. Khoshnejad, M., Shuvaev, V.V., Pulsipher, K.W., Dai, C., Hood, E.D., Arguiri, E., Christofidou-Solomidou, M., Dmochowski, I.J., Greineder, C.F., and Muzykantov, V.R. (2016). Vascular Accessibility of Endothelial Targeted Ferritin Nanoparticles. *Bioconjug. Chem.* 27, 628–637.